The Automatic Polar Map Creation for Myocardial Perfusion SPECT Analysis Using Image Registration Combined with Feature Extraction

Gabriel Paniz Patzer[1], Marcelo Zanchetta do Nascimento[2], Marcus Vínicius Simões[3], Jeovane Honório Alves[4], Lauro Wichert-Ana[3], Paulo Mazzoncini de Azevedo-Marques[3], Lucas Ferrari de Oliveira[4]

[1] Anglican University of Erechim (FAE)
Av. Sete de Setembro, 44 – CEP 99700-300
Erechim (RS) – Brazil

[2]Federal University of Uberlândia (UFU)
Av. João Naves de Ávila 2121 – Campus Santa Mônica
CEP 38408-100 – Uberlândia (MG) – Brazil

[3]University of São Paulo (USP)
Av. Bandeirantes, 3900 – Monte Alegre – CEP: 14049-900
Ribeirão Preto (SP) – Brazil

[4]Federal University of Paraná (UFPR)
R. Cel. Francisco H. dos Santos, 100 Centro Politécnico
Jardim das Américas – CEP: 81531-980 – Curitiba (SP) – Brazil

lferrari@ufpr.br

Abstract. *This paper describes a technique for an automatic polar map creation from myocardial perfusion SPECT images. This exam is widely used in post-infarction patient evaluations, in order to foretell the outcome and left ventricular function. This exam is difficult to interpret, since it is a 3D representation of the heart. Use of polar maps intends to simplify analysis of the exam, converting the 3D image into a 2D plot. The technique developed is based on a combination of image registration and feature detection. For this study, an overall of 31 cases were tested, with the results compared with the gold standard software. The correlation calculated between techniques was 0.76 in the worst case and 0.98 in the best case.*
Index Terms: Image Registration, Myocardial Infarction, Polar Map, SPECT.

1. Introduction

Considered the most severe clinical syndrome related to ischemic disease of the heart, Acute Myocardial Infarction (AMI) is responsible for 25% of deaths registered in the United States, representing an absolute number of approximately 1.1 million cases every year. In England, there is an estimated incidence of 2.6 deaths per one thousand inhabitants a year [Birkhead et al. 1999, Pope et al. 2000]. Patients that survive an AMI might be in a risk zone, in which there is a possibility of recurrent infarction and even death in the first several months after hospital discharge. Several clinical and laboratory factors are used to predict patients condition post-AMI, in order to identify whether they are inside the risk zone [Group et al. 1983]. Combination of necrotic tissue with viable tissue determines the extension of myocardial dysfunction, in other words, ischemia resulting in malfunction of the cardiac muscle [Group et al. 1983]. Nuclear medicine exams, such as Single Photon Emission Computed Tomography (SPECT), represents a non-invasive technique for determining capability of perfusion of the myocardium [Barros et al. 2007]. However, this type of exam may be difficult to interpret, as its image presents low spatial resolution and it is a three-dimensional representation composed of dozen plane images. SPECT images have 64x64 pixels or 128x128 pixels in long axis, in general, and approximately 40 slices in short axis. A polar map is the easiest way to facilitate its visualization and interpretation [Oliveira et al. 2007].

The technique of polar map, also known as bull's-eye map, is a method standardized to inspect the heart areas, generating a plane representation of the left ventricular wall [DePuey et al. 2001, Dvorak et al. 2011]. The technique can be used to evaluate the denervation of Left Ventricle (LV) as well as show the abnormal left ventricular myocardial perfusion [Dvorak et al. 2011, Ohshima et al. 2013]. Inherent difficulty in polar maps' construction is the downside of this technique, which requires manual orientation of structures in volumetric space by a specialist. Heart structures must be correctly adjusted for the process to be successful, allowing the polar map to represent heart regions correctly. Aiming to reduce the level of uncertainty in this task, this study applies image registration techniques to automatize the construction process of polar maps without specialist intervention. Registration methods are used to geometrically transform the analyzed image, aligning it spatially to a model image [Hill et al. 2001].

Due to cardiac images' characteristics and factors inherent to the alignment process, the most disseminated alignment techniques (cross-correlation, mutual information and normalized mutual information) present a result below the expectation when used for SPECT-SPECT alignment [Barros et al. 2007, DePuey et al. 2001, Makela et al. 2002, Oliveira et al. 2007]. The problem on this kind of alignment is due to the short axis, since it directly influences the polar map and because, in several cases, the right ventricle is not represented completely, complicating the use of an automated registration algorithm [Barros et al. 2007].

This study proposes a hybrid methodology that combines algorithms of image registration based on voxel intensity with a technique for texture feature extraction. These two approaches were applied, the first for the long axis and the second for short axis alignment. The present study proposes an algorithm for automatic alignment of myocardial scintigraphy exams, allowing the creation of polar maps without specialist intervention.

2. Methods

2.1. Templates used in alignment

For the application of the alignment stage, templates proposed by [Pádua et al. 2008] were used in an attempt to reduce uncertainty of heart areas' position and improve automation of the process. Templates were built from 20 images of patients, 10 male and 10 female, with approximated weight and height (in rest condition, obtained from volunteers without cardiac defect). The voxel values of the images were normalized on a percentile scale, from 0 to 100, aligned semi-automatically with use of VTK CISG Registration Toolkit (supervised and validated by a specialist) and aligned images were added to each other, creating two templates [Hartkens et al. 2002].

Coordinates (x,y,z) demarcating apical and base-mid ventricular areas were defined on the templates. These definitions were used in other stages to create the polar map.

2.2. Case Study

Images used in this study were provided by the Medical School of Ribeirão Preto, University of São Paulo (HCFMRP/USP), using anonymous data of the patients. These images were obtained with a digital scintillation camera (Sopha Medical Vision) equipped with a double detector and a low energy parallel collimator. Sestamibi labeled with Tc-99m was used as myocardial perfusion tracer. The protocol of imaging included a rest-stress sequence with injected doses of radiotracer of 8 mCi at rest and 25 mCi at peak stress. Energy window used was 20%, centered in 70 keV. Tomographic plans were obtained in circular orbit, covering 180º, including 32 projections (16 per detector) with 60 seconds of duration per projection. Reconstruction of these images were done by the proprietary software associated with the acquisition equipment.

After the reconstruction stage, the images were filtered by the specialist using the acquisition equipment, through a Butterworth filter for enhancement, with the parameters of order = 5 and cut frequency = 0.25 cy/mm. Tomographic slices in classic orthogonal plans were generated by proprietary software, with positioning performed by a specialist. DICOM standard was used to store these images.

The protocol followed for acquisition of the images was stress based, with administration of a radiotracer to the patients while they were performing physical exercise. Images provided by the HCFMRP-USP constitute a database of cases obtained from 31 patients, organized into 2 classes:

- 18 cases of female patients (12 with cardiac lesion and 6 without lesion);
- 13 cases of male patients (10 with cardiac lesion and 3 without lesion);

For each case, there are approximately 50 images of 64x64 pixels.

2.3. Image Registration Techniques

2.3.1. Scale and Translation Registration

In this step, the dimensions and spatial positioning of the patients' images were adjusted to the template, thus creating a spatial standardization.

The main objective was the centralization of the left ventricular cavity. In order to have each rotation over an axis applied correctly, it was necessary to know a priori the correct positioning of that axis. Size of the myocardium may influence the creation of the polar map and this parameter varies according to the patient's weight, size and sex. In this case, the alignment technique aims to approximate the analyzed exam to the one represented by the template image.

For the alignment algorithm, the mutual information similarity measurement was used between the template and the patients' images. Mutual information is given by equation (1).

$$I(X,Y) = H(X) + H(Y) - H(X,Y) \tag{1}$$

in which $H(.)$ is the entropy of the image X or Y, $H(X, Y)$ is the joint entropy of the images. In case a similarity threshold is not reached, the algorithm applies a new transformation (scale and translation), using a method of optimization based on gradient descent of the similarity value in the analyzed image. Optimization procedure is performed until the acceptance margin is achieved or until 200 iterations have occurred.

2.3.2. Long Axis Registration

The next step was necessary to correct the orientation through rotation transformations, since the myocardium was already in the correct position. Mutual information was used as a similarity measure, but the transformations applied are only made at the rotation of both long axis.

The optimization method determined which long axis, direction and degree of transformation should be applied to the image. After applying the transformation to the target image, similarity measure was calculated again and the process was repeated. The method only stopped when it achieved an adequate similarity value or its maximum number of iterations.

2.3.3. Short Axis Registration

In the previous stages of alignment, the image was analyzed as a whole 3D volume. For the short axis alignment stage, only some slices (2D) were inspected to determine the correct rotation to be applied on the volume. For the tests performed, the alignment algorithms, through similarity measure, could not determine precisely the inferior junction between right and left ventricles. In his study, [Nekolla et al. 1998] proposed a technique that used isosurfaces to determine the positioning of the inferior junction. In some cases, the images were cutted and reference points were lost, affecting the detection.

Due to this problem, generated polar maps did not present same conformation and they were often rotated at the short axis. In an attempt to solve this problem, an alignment algorithm based on feature extraction was applied, more specifically the Scale-Invariant Feature Transform technique (SIFT). This technique detects points, in both the templates and base images, in order to approximate the information present in the image [Lowe 2004].

SIFT generates an array of affine transformation invariant descriptors associated with keypoints selected in the image using different algorithms. Each slice is scaled to double its size using bicubic interpolation and blurred by a Gaussian filter with five different levels (with increasing degrees of blur) to get keypoints' candidates. SIFT determines key-points through the Difference of Gaussians from images in different levels of samples [Lowe 2004].

From the analysis of the points detected in the images, the rotation correction may be performed based only on the central region of the left ventricle. For the algorithm of alignment of the short axis, the first step was to select the slice in which the left ventricle was evidenced. Due to SPECT images' low resolution, 64x64 pixels in general, few points were found in some cases. In order to improve performance of point detection, the image was resized to 128x128 pixels, using bicubic interpolation [Gonzalez 2007].

The template images were analyzed by specialists to determine the slice representing the best distribution of information. Due to the template's alignment, it is possible to state that the same structures were represented in the same slice of the short axis in both images. The slice chosen was the number 35, from a total of 47 slices, because of the evident presence of the inferior junction, the largest cavity of the left ventricle, and also due to a lesser portion of the image as background. For the feature extraction, SIFT was applied to the slice and, in case the technique failed to find the central point of the myocardium, adjoining slices were analyzed and SIFT was applied again until the process was successful in determining the object of interest.

After finding the central point in the patient's image, the algorithm also determined its orientation, and compared it to the orientation of the central point in the template image. The difference between the orientations determines the angle of the rotation transformation to be applied in the short axis to execute the final alignment of the image. Figure 1 shows the orientation of the central point in an analyzed image and in the template image. Highlighted points in the center of the images indicate the position and orientation detected by the SIFT technique for a certain point of the analyzed image (see Figure 1-A) and the corresponding one in the template image (see Figure 1-B). The technique works automatically without intervention of specialists.

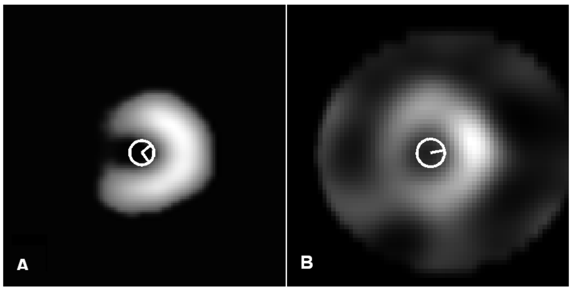

Figure 1. Left Ventricle slice with central key point, selected by the SIFT technique. In A the patient with SIFT key points and in B the template orientation.

2.4. Polar Map Generation

The polar map technique was originally developed at the University of Emory by [Garcia et al. 1985]. This technique aims to reduce the complexity of visualization of the three-dimensional images produced by the SPECT exam. Representation of the images of 3D scintigraphy is made in only one bi-dimensional image that outlines the perfusion in the left ventricle [Dvorak et al. 2011].

Polar maps are easily interpretable images, providing information on the perfusion of the whole left ventricle, from apex to base. In a single image, they permit the assessment of relative perfusion of individual walls and analysis of perfusion defects' extent. Besides, generation of polar maps from SPECT studies allows inter-patient comparisons as well as with normality models [DePuey et al. 2001].

A polar map describes the perfusion defect in terms of extent (small, medium and large), severity, reversibility (reversible, fixed or mixed) and localization [Fathala 2011].

To analyze regional left ventricular function, the most adopted standard model is the 17-myocardial segment, recommended by American Heart Association in 2002 [Cerqueira et al. 2002]. In this model, individual segments were assigned to coronary artery territories and it was used in this work to compare the methodology proposed with the gold standard [Donato et al. 2012].

A selection of points of maximum uptake in regions is used to create a polar map, obtained by the search angle, from the center of the left ventricule of known size [DePuey et al. 2001]. This region size varies according to the technique. The angle of 6^o is normally used according to the original technique developed by [Garcia et al. 1985], and 10^o is used in the technique of the Cedars-Sinai Center [DePuey et al. 2001].

Generation of polar map involves abstraction of the heart shape in simpler geometrical shapes. In this work, a cylinder was used to represent the base and the body of the left ventricle. For the peak of the myocardium, a semi-spherical sampling was used, this technique was proposed by [Oliveira et al. 2007]. In both abstractions, the search angle was 1^o and the resulting polar map was blurred through a Gaussian Filter to smooth its appearance and eliminate noise. According to [Lin et al. 2006], polar maps generated using different types of abstraction are not comparable. Therefore, the methods use a convention for polar map orientation, in which the myocardium is represented from the bottom up, starting at the peak and with the walls: anterior aspect of the left ventricule in the superior section and septal to the right.

3. Results

For each one of 17-myocardial segments, the mean values of these pixels were calculated and compared with the region values provided by gold standard software. Figure 2 shows the location of the segments in the polar maps.

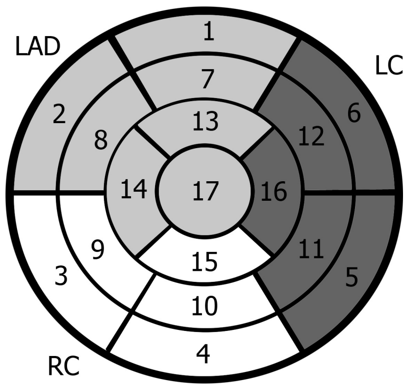

Figure 2. The 17-myocardial segments used in this work.

The Pearson's correlation coefficient was used to verify the correspondence between the proposed methodology and the gold standard, on each segment for each patient. The patients groups were described in 2.2 section. The two patients groups were analyzed separately and the average and standard deviation from correlations coefficients were calculated between the groups.

The Tables 1 and 2 present the correlation values for each genre group. The mean correlation and the standard deviation is shown in the end of the tables. Analyzing the female group in the Table 1, the worst correlation was in the patient #3 with 0.76 and the best was patient #18 with 0.98. The mean correlation was 0.93 and the standard deviation 0.05.

Table 1: Female Patients Results

Patient	1	2	3	4	5	6	7	8	9	10	11	12	13	14	15	16	17	18
Corre-lation	0.92	0.95	0.76	0.96	0.97	0.85	0.97	0.88	0.97	0.93	0.98	0.95	0.96	0.91	0.95	0.94	0.92	0.98
Mean	0.93																	
SD	0.05																	

Table 2: Male Patients Results

Patient	1	2	3	4	5	6	7	8	9	10	11	12	13
Corre-lation	0.95	0.94	0.93	0.95	0.98	0.94	0.90	0.95	0.96	0.96	0.95	0.88	0.97
Mean	0.94												
SD	0.03												

In Figure 3, eight Polar Maps from four patients (two normal and two ischemic) were showed, on the top two Female patients (#3 and #17) in A the maps created using our technique and in B the gold-standard software. On the bottom, two male patients (#11 and #2). In these images it is possible to perceive the pixel difference between the created maps (more smooth in our technique).

To verify the similarity the null hypothesis (H_0) was tested using the Student's *t*-test within all patients (male and female) and the two maps (gold standard and proposed technique) created. For each patient the paired *t*-test two tailed was calculated ($P < 0.001$). In all cases the null hypothesis was accepted, the highest *t*-test value was 0.7918 and the smallest was 0.00015. Hence, there wasn't statistical difference between the technique developed and the gold standard.

4. Discussion

Techniques of image alignment that use the similarity of voxels became more evident in the last few years due to the results presented. The image alignment using a model is useful for the definition of regions of the studied object.

In tests performed by [Pádua et al. 2008], the images had to be corrected manually by a specialist, since the objective was to create templates that would represent the mean of functional activity among normal patients. This means that templates were useful for the present study, but the methodology of alignment had to be modified, because the inferior junction of the left to the right ventricle was not correctly adjusted, and the polar map created had a rotated aspect compared to the gold standard. The alignment of the long and short axis using the mutual information as a measure of voxel similarity in the operations of scale, translation and rotation showed that every operation was correctly performed, with exception to the rotation in the short axis. Therefore, it was necessary to find a new approach for the short axis.

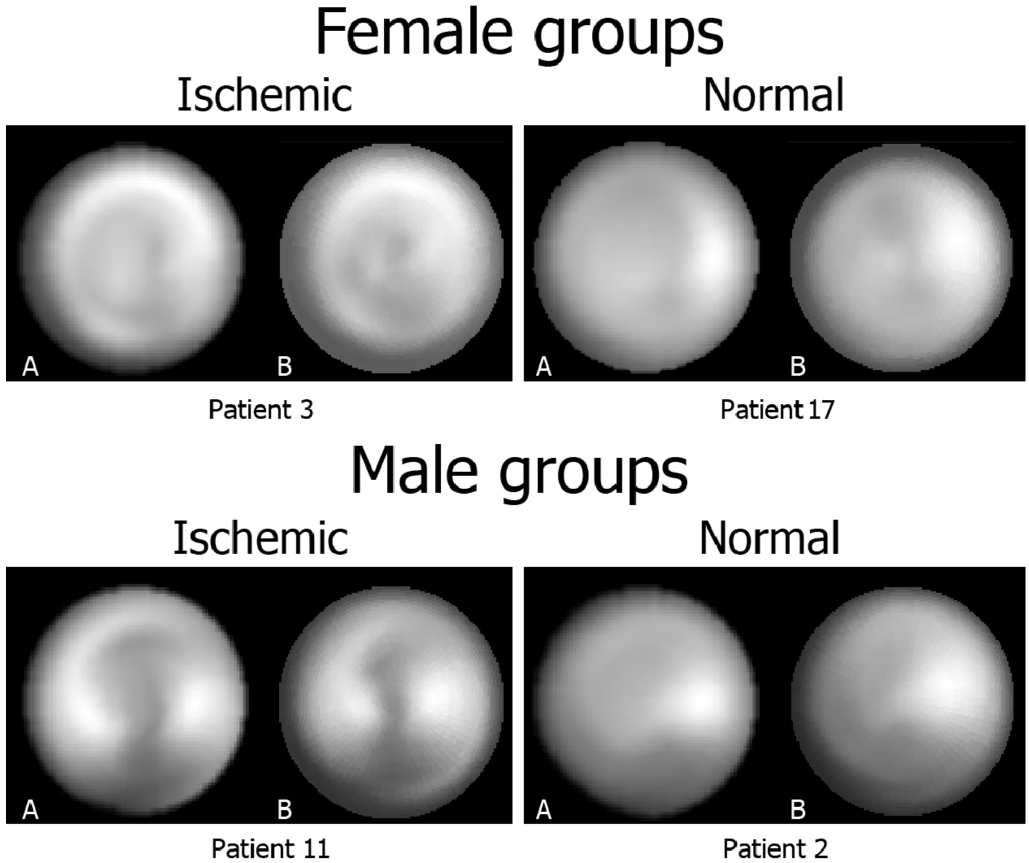

Figure 3. Comparison between polar maps created with the proposed technique (marked as A) and the gold standard software (marked as B).

The SIFT technique for the detection of key points was used to detect the central point of the myocardium and its orientation using a 2D image. This stage was found to be efficient, but it was necessary to double the image size to find the control points. Use of the SIFT technique allowed a satisfactory alignment of the inferior junction of the left ventricle, so the patient's image could be adjusted to the proposed templates. The results presented a high level of correlation, with an average of 93% between the proposed methodology and the gold standard. However, some regions presented error value due to the sampling difference.

All the tools used in the quantization of SPECT studies, like QGS and Emory Cardiac Toolbox, are proprietary software, elevating the total cost of this type of solution [Lin et al. 2006]. Our goal is to develop and distribute the software as free software, making possible its modification according to the particular needs of each institution, reducing the total cost of the solution.

5. Conclusion

This study presents a new proposal for alignment of cardiac SPECT images and automatic generation of polar maps. In order to validate the methodology proposed, an image dataset with 31 exams was used (18 females and 13 males), with and without ischemic injury. It was processed by a specialist in proprietary software, and polar maps were created using the proposed technique. These maps were compared using Pearson's coefficient of correlation and the similarity was tested by paired *t*-tests in the 17 segments.

The better representation of the shape of region was the semi-spherical sampling of the myocardium apex. However, in comparison with the gold standard method, the results were slightly worse in the female groups. This difference is probably due to the shape of the male myocardium, which is more rounded at the cardiac apex, and the differentiated sampling. It is worth highlighting the sample results cannot be directly compared. Instead, the correlation and similarity between them were analyzed, since the samples are made differently. However, the correlation between the techniques showed that, even being made differently, the results presented are coherent among themselves. The hypothesis Student *t*-test did not present statistical difference among the 17-segments' averages, thus supporting the conclusion of consistency between techniques.

References

Barros, R. C., Oliveira, L. F., and Simões, M. V. (2007). Quantitative analysis of spect myocardial perfusion and assessment of myocardium defect regions through image processing techniques. In *XX Brazilian Symposium on Computer Graphics and Image Processing, Technical Poster session*, pages 51–52.

Birkhead, J., Goldacre, M., Mason, A., Wilkinson, E., Amess, M., Cleary, R., and editors (1999). Health outcome indicators: Myocardial infarction. report of a working group to the department of health. Technical report, Oxford: National Centre for Health Outcomes Development.

Cerqueira, M. D., Weissman, N. J., Dilsizian, V., Jacobs, A. K., Kaul, S., Laskey, W. K., Pennell, D. J., Rumberger, J. A., Ryan, T., Verani, M. S., et al. (2002). Standardized myocardial segmentation and nomenclature for tomographic imaging of the heart a statement for healthcare professionals from the cardiac imaging committee of the council on clinical cardiology of the american heart association. *Circulation*, 105(4):539–542.

DePuey, E. G., Garcia, E. V., and Berman, D. S. (2001). *Cardiac SPECT imaging*. Lippincott Williams & Wilkins.

Donato, P., Coelho, P., Santos, C., Bernardes, A., and Caseiro-Alves, F. (2012). Correspondence between left ventricular 17 myocardial segments and coronary anatomy obtained by multi-detector computed tomography: an ex vivo contribution. *Surgical and radiologic anatomy*, 34(9):805–810.

Dvorak, R. A., Brown, R. K., and Corbett, J. R. (2011). Interpretation of spect/ct myocardial perfusion images: common artifacts and quality control techniques. *Radiographics*, 31(7):2041–2057.

Fathala, A. (2011). Myocardial perfusion scintigraphy: techniques, interpretation, indications and reporting. *Annals of Saudi medicine*, 31(6):625.

Garcia, E. V., Van Train, K., Maddahi, J., Prigent, F., Friedman, J., Areeda, J., Waxman, A., and Berman, D. S. (1985). Quantification of rotational thallium-201 myocardial tomography. *Journal of Nuclear Medicine*, 26(1):17–26.

Gonzalez, R. C. (2007). Digital image processing author: Rafael c. gonzalez, richard e. woods, publisher: Prentice hall pages: 976 p.

Group, M. P. R. et al. (1983). Risk stratification and survival after myocardial infarction. *N Engl J Med*, 309:331–336.

Hartkens, T., Rueckert, D., Schnabel, J. A., Hawkes, D. J., and Hill, D. L. (2002). Vtk cisg registration toolkit an open source software package for affine and non-rigid registration of single-and multimodal 3d images. In *Bildverarbeitung für die Medizin 2002*, pages 409–412. Springer.

Hill, D. L., Batchelor, P. G., Holden, M., and Hawkes, D. J. (2001). Medical image registration. *Physics in medicine and biology*, 46(3):R1.

Lin, G. S., Hines, H. H., Grant, G., Taylor, K., and Ryals, C. (2006). Automated quantification of myocardial ischemia and wall motion defects by use of cardiac spect polar mapping and 4-dimensional surface rendering. *Journal of nuclear medicine technology*, 34(1):3–17.

Lowe, D. G. (2004). Distinctive image features from scale-invariant keypoints. *International journal of computer vision*, 60(2):91–110.

Makela, T., Clarysse, P., Sipila, O., Pauna, N., Pham, Q. C., Katila, T., and Magnin, I. E. (2002). A review of cardiac image registration methods. *Medical Imaging, IEEE Transactions on*, 21(9):1011–1021.

Nekolla, S. G., Miethaner, C., Nguyen, N., Ziegler, S. I., and Schwaiger, M. (1998). Reproducibility of polar map generation and assessment of defect severity and extent assessment in myocardial perfusion imaging using positron emission tomography. *European Journal of Nuclear Medicine*, 25(9):1313–1321.

Ohshima, S., Isobe, S., Hayashi, D., Abe, S., Kato, K., and Murohara, T. (2013). Myocardial 123i-mibg scintigraphy predicts an impairment in myocardial functional reserve during dobutamine stress in patients with idiopathic dilated cardiomyopathy. *European Journal of Nuclear Medicine and Molecular Imaging*, 40(2):262–270.

Oliveira, L. F., Zanchet, B. A., Barros, R. C., and Simões, M. V. (2007). A new approach for creating polar maps of three-dimensional cardiac perfusion images. In *XX Brazilian Symposium on Computer Graphics and Image Processing,*.

Pope, J. H., Aufderheide, T. P., Ruthazer, R., Woolard, R. H., Feldman, J. A., Beshansky, J. R., Griffith, J. L., and Selker, H. P. (2000). Missed diagnoses of acute cardiac ischemia in the emergency department. *New England Journal of Medicine*, 342(16):1163–1170. PMID: 10770981.

Pádua, R. D. S., Oliveira, L. F., Azevedo-Marques, P. M., Groote, J.-J. G. S., Castro, A. A., Wichert-Ana, L., and Simões, M. V. (2008). Aid in the detection of myocardial perfusion abnormality utilizing SPECT atlas and images registration: preliminary results. *Radiologia Brasileira*, 41:397 – 402.